
Plasma Measurements for JET

P. E. Stott

Phil. Trans. R. Soc. Lond. A 1987 **322**, 47-65

doi: 10.1098/rsta.1987.0037

Email alerting service

Receive free email alerts when new articles cite this article - sign up in the box at the top right-hand corner of the article or click [here](#)

To subscribe to *Phil. Trans. R. Soc. Lond. A* go to: <http://rsta.royalsocietypublishing.org/subscriptions>

Plasma measurements for JET

BY P. E. STOTT

JET Joint Undertaking, Abingdon, Oxfordshire OX14 3EA, U.K.

An important requirement for fusion experiments like JET is the accurate and reliable measurement of the plasma parameters. The most important quantities to be measured include the discharge current, the position and shape of the plasma boundary, the densities and temperatures of the ions and electrons, the concentrations of impurity ions and the various energy input and loss mechanisms. Because all of these quantities vary in space and time, a large number of measurement channels is needed, and a large amount of data is generated for each discharge.

Measurements in high-temperature plasmas are difficult because material probes cannot be used except at the extreme edge of the discharge. For measurements in the hot central regions, non-material probes based on electromagnetic radiation or particle beams are used together with analysis of electromagnetic radiation and particles emitted spontaneously from the plasma. A wide variety of experimental techniques is utilized and the application of some of these methods to JET will be described.

INTRODUCTION

An important requirement for a fusion experiment like JET is the accurate and reliable measurement of the plasma conditions. In a magnetically confined plasma there are many quantities to be measured to characterize the plasma and to compare experiment with theory. The most important quantities which are measured in JET include macroscopic parameters like the plasma position, shape, current, energy content, and spatially varying quantities like the densities and temperatures of each of the component species (i.e. electrons, hydrogenic ions and impurity ions). Some of these quantities (current, position, shape and density) are measured in real time and included in feedback loops to control the discharge.

Measurements in high temperature plasmas are difficult because material probes cannot be used except at the extreme edge where the plasma is sufficiently cool (not more than about 100 eV). For measurements in the hotter core of the plasma non-invasive techniques are required. These include passive methods that detect radiation or particles emitted spontaneously by the plasma and active methods where radiation or particles from an external source are used to probe the plasma. Many techniques make use of electromagnetic radiation and the spectral range covered in JET is shown in figure 1. Use is also made of charged and neutral particles and neutrons.

In attempting to review these plasma measurement systems (or diagnostics as they are commonly called) in a systematic way, they can be grouped either according to the measurement technique (e.g. laser scattering, X-rays) or according to the plasma parameter which is to be measured (e.g. density, temperature). Neither classification method can be followed completely systematically because many measurement methods, in fact, give information on more than one plasma parameter, and conversely we usually use more than one method to measure each of the more important parameters. This overlap is very important

Spectrum covered by JET diagnostics

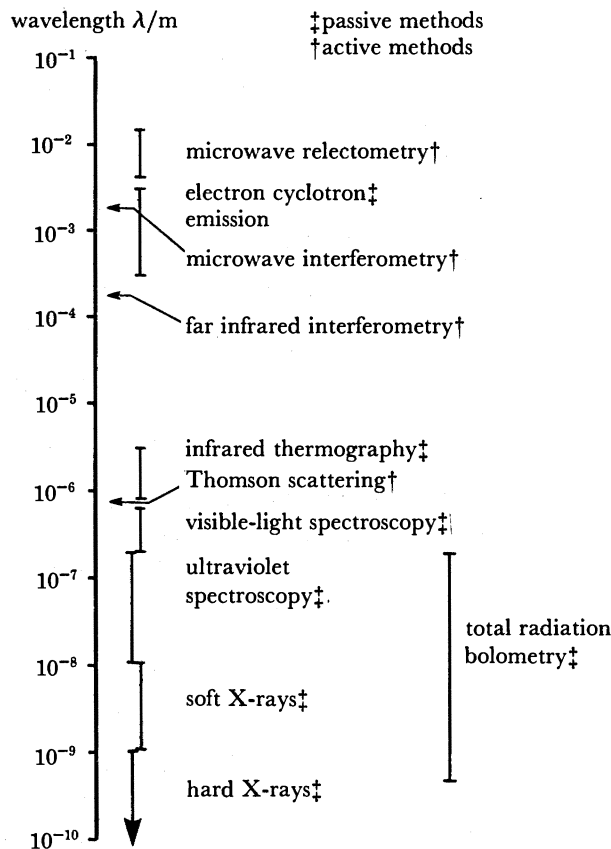


FIGURE 1. Spectral range covered by JET diagnostics. \dagger , Active methods; \ddagger , passive methods.

for reliability and confidence in the measurements. It is important to stress that this duplication is needed not because the diagnostic equipment is unreliable but because in many cases the measurements themselves rely on complicated plasma physics effects whose interpretation may not always be straightforward. For example, some of the measurement methods need cross calibration against other measurements, some are restricted to certain ranges of plasma parameters and to cover the whole operating range of JET may be outside the scope of a single method, and in some cases there may be competing plasma effects, which could confuse the interpretation. Clearly the accuracy of the measurements is important, particularly because most of the basic data are used to derive other plasma quantities, and therefore inaccuracies or errors in basic quantities can propagate down the entire analysis chain. It is generally accepted that most plasma measurements are accurate only to within $\pm 20\%$, but by careful design and calibration we have been able to improve on this in JET (for example in the measurement of electron temperature) as will be discussed below.

The total number of diagnostic systems installed or being built for JET is around 30 and their present status is summarized in table 1. A schematic layout is shown in figure 2. It will be seen that many of these systems have been built by the other fusion laboratories who are partners in the JET project. These systems have been specified and paid for by the JET project via a series of contracts placed with these other laboratories. This formal relation was needed

TABLE 1. STATUS OF THE JET DIAGNOSTICS SYSTEMS

diagnostic system	diagnostic	purpose	association	status December 1985	date of operation in JET
KB1	bolometer scan	time and space resolved total radiated power	IPP, Garching	operational	mid 1983 partly early 1984 fully
KC1	magnetic diagnostics	plasma current, loop volts, plasma position, shape of flux surfaces	JET	(1) operational (2) enhancement	mid 1983 late 1985
KE1	single point Thomson scattering	T_e and n_e at one point several times	Riso	operational	mid 1984
KE3	Lidar Thomson scattering	T_e and n_e profiles	JET and Stuttgart University	construction	early 1987
KG1	multichannel far-infrared interferometer and polarimeter	(1) $\int n_e ds$ on 7 vertical chords and 3 horizontal chords (2) $\int n_e B_p ds$ on 6 vertical chords	CEA, Fontenay-aux-Roses	(1) operational (2) under construction	mid 1984 partly early 1985 fully
KG2	single channel microwave	$\int n_e(r) ds$ on 1 vertical and 3 horizontal chords in low-density plasmas ($< 10^{20} m^{-3}$)	JET and FOM, Rijnhuizen	2 mm operational	early 1987 mid 1983
KG3	microwave reflectometer	n_e profiles and fluctuations	JET	(1) prototype system operating (2) multichannel system being designed	mid 1983 mid 1987 mid 1983
KH1	hard X-ray monitors	runaway electrons and disruptions	JET	operational	mid 1983
KH2	X-ray pulse height spectrometer	plasma-purity monitor and T_e on axis	JET	installed	early 1986
KJ1	soft X-ray diode arrays	MHD instabilities and location of rational surfaces	IPP, Garching	operational	end 1985
KK1	electron-cyclotron emission spatial scan	$T_e(r,t)$ with scan time of a few milliseconds	NPL, Culham Laboratory and JET	operational	late 1985
KK2	electron-cyclotron emission fast system	$T_e(r,t)$ on microsecond time scale	FOM, Rijnhuizen	operational	early 1985
KL1	limiter surface temperature	(i) monitor of hot spots on limiter and RF antennas (ii) temperature of wall and limiter surface	JET and KFA, Jülich	operational development	mid 1984 1986
KM1	2.4 MeV neutron spectrometer	neutron spectra in D-D discharges, ion temperatures and energy distributions	UKAEA, Harwell	construction proceeding	1986
KM3	2.4 MeV time-of-flight neutron spectrometer		SERC, Studsvik	commissioning	1986
KM4	2.4 MeV spherical ionization chamber		KFA, Jülich	commissioning	1986
KM2	14 MeV neutron spectrometer		UKAEA, Harwell	design completed	
KM5	14 MeV neutron spectrometer	neutron spectra in D-T discharges, ion temperatures and energy distributions	SERC, Gothenberg	decision on construction under review	
KN1	time-resolved neutron-yield monitor	time-resolved neutron flux	UKAEA, Harwell	operational	mid 1983
KN2	neutron activation	absolute fluxes of neutrons	UKAEA, Harwell	installation	1986
KN3	neutron-yield profile-measuring system	space- and time-resolved profile of neutron flux	UKAEA, Harwell	construction proceeding	1986
KN4	delayed neutron activation	absolute fluxes of neutrons	Mol	awaiting delivery	1986
KP1	fusion product detectors	charged particles produced by fusion reactions	JET	prototype operational upgrade	1985 1986
KR1	neutral-particle analyser array	profiles of ion temperature	ENEA, Frascati	operational	mid 1984 partly end 1985 fully
KS1	active-phase spectroscopy	impurity behaviour in active conditions	IPP, Garching	under construction	mid 1986
KS2	spatial scan X-ray crystal spectroscopy	space- and time-resolved impurity density profiles	IPP, Garching	under construction	early 1986
KS3	H α and visible light monitors	ionization rate, Z_{eff} , impurity fluxes	JET	operational	early 1983 early 1986
KS4	active beam diagnostics (with heating beam)	fully ionized light-impurity concentration $T_i(r)$ rotation velocities	JET	provisional system under construction	early 1986 early 1987
KT1	VUV spectroscopy spatial scan	time- and space-resolved impurity densities	CEA, Fontenay-aux-Roses	operational	mid 1985
KT2	VUV broadband spectroscopy	impurity survey	UKAEA, Culham Laboratory	operational	early 1984
KT3	visible spectroscopy	impurity fluxes from wall and limiters	JET	operational	mid 1983
KT4	grazing incidence spectroscopy	impurity survey	UKAEA, Culham Laboratory	under construction	early 1986
KX1	high resolution X-ray crystal spectroscopy	ion temperature by line broadening	ENEA, Frascati	installed	early 1986
KY1	surface analysis station	plasma-wall and limiter interactions including release of hydrogen isotope recycling vertical probe drives for electrical and surface collecting probes	IPP, Garching	commissioning	mid 1986
KY2	surface probe fast-transfer system		UKAEA, Culham Laboratory	commissioning	mid 1986
KY3	plasma-boundary probe		JET UKAEA, Culham Laboratory	both units installed	mid 1984-86
KZ1	pellet injector diagnostic	particle transport, fuelling	IPP, Garching	partly installed	early 1986

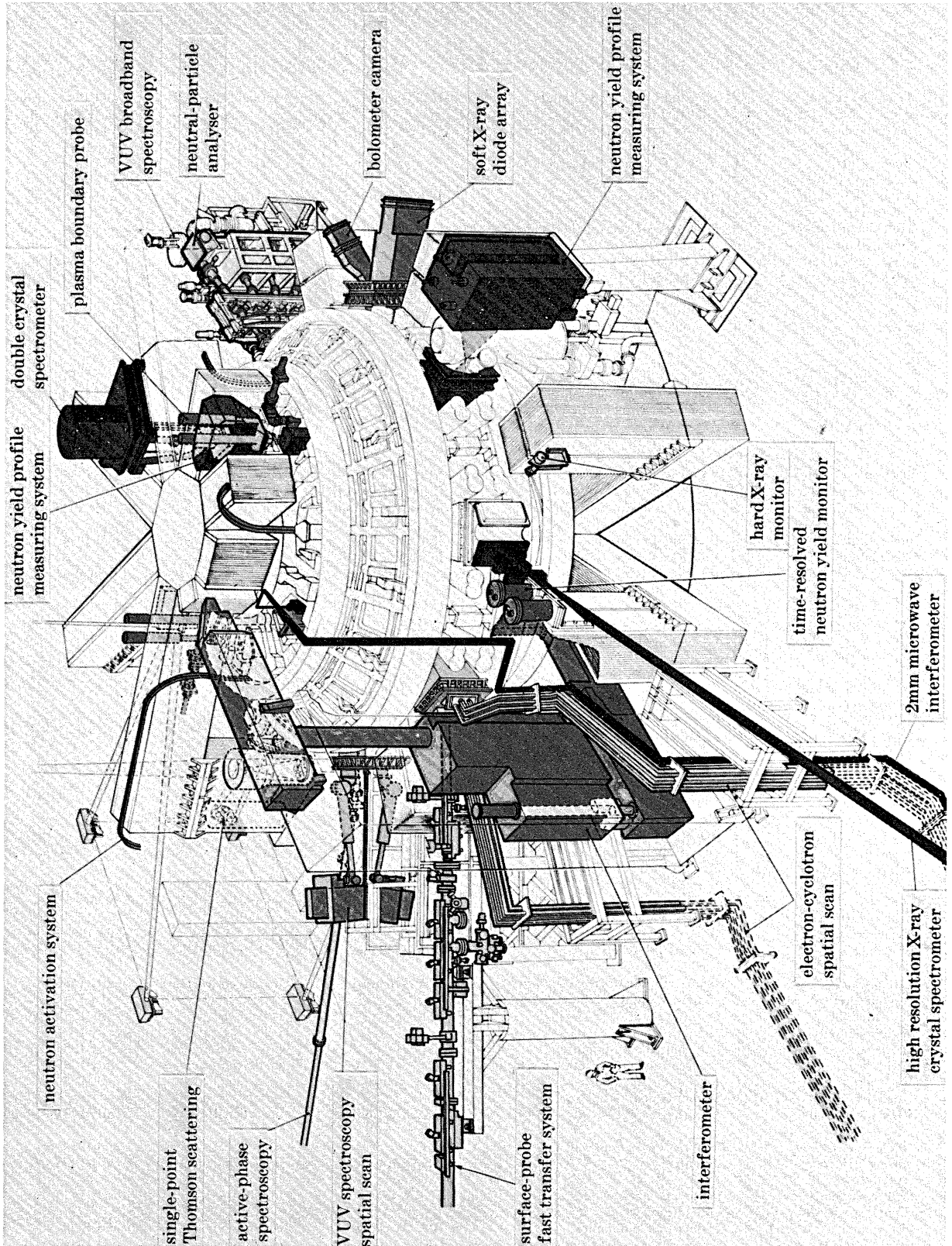


FIGURE 2. Schematic showing the location of JET diagnostic systems.

so that the work in the many different laboratories could be effectively coordinated and the complex systems could be built to uniform standards. This has been a particularly successful collaboration with the result that the diagnostic expertise of the European fusion programme has been concentrated in JET. Many skilled scientists, engineers and technicians have been involved and many of these have worked at JET for varying periods to install or operate these systems.

A deliberate policy has been to use diagnostics methods whenever possible whose principles have been demonstrated on other experiments. What is new in JET is the sophistication of the application of these methods and the complexity of the engineering. This has been necessitated by several factors including the large physical size of JET, the need to maintain compatibility with the very high standards of engineering on all other systems of the JET device, and by the hostile radiation environment that will occur in discharges with deuterium and tritium. Considerable emphasis has been placed on achieving much higher standards of reliability for the diagnostic systems than has previously been the norm in fusion research. All of the JET diagnostic systems are remotely controlled through a computer system and the more important diagnostics can be operated automatically with a minimum of skilled operators.

To make the most effective use of experimental time on JET and to improve the self-consistency of the data, a complete set of data is measured simultaneously on every discharge. In general we find that the measurements are reproducible from shot to shot for discharges with the same conditions. A large number of spatial channels is needed to measure profiles of plasma parameters with adequate spatial resolution (generally 5–10 cm) in these discharges with large poloidal cross section ($2.5 \text{ m} \times 4.2 \text{ m}$). As the poloidal cross section is non-circular, those measurements that integrate along a chordal line of sight have to be unfolded by tomographic inversion methods and thus the plasma must be viewed in orthogonal directions. In most cases the number and locations of the lines of sight are severely constrained by the access to the plasma through the available ports in the vacuum vessel. There are similar considerations in determining the time scales on which data should be recorded. The plasma parameters related to quasi-equilibrium processes (e.g. energy balance) need to be recorded on time scales up to an order of magnitude shorter than the characteristic equilibrium times, e.g. recording on time scales of *ca.* 10 ms is required for equilibrium times *ca.* 100 ms. Data are usually recorded at this rate throughout the 20 s JET discharge, i.e. about 2×10^3 data points per channel. There are, however, many transient plasma phenomena that take place on much shorter time scales (e.g. instabilities and disruptions) and these data must be recorded on time scales of a few microseconds. Clearly it would be impractical in terms of data storage to record data on all the measurement channels at this rate throughout the JET discharge and so the fastest data-taking rate is usually switched on for a limited number of time windows centred around the periods of interest in the discharge. These windows may be pre- or post-triggered in some cases by signals from other diagnostics.

Fairly stringent constraints have had to be applied to the data requirements of each diagnostic to keep the total data recorded per JET discharge within reasonable limits. Now we record *ca.* 7×10^6 data points per discharge and this is expected to increase to *ca.* 1.5×10^7 when all planned diagnostics are operating. The data are recorded in local CAMAC memory during the discharge, and then read into the memory of one of a network of computers used for diagnostic and machine control and for data analysis. Initial analysis and display of results is carried out by these computers in the period between discharges and is used as a guide to

the progress of the experiment. At the same time the complete raw-data file is copied into the memory of a large mainframe computer where it can be used for higher-level analysis and it is via this computer that retrospective analysis of JET data is carried out. An important feature of JET is that data for all JET discharges and from all the JET diagnostics is available to all of the JET team on this mainframe computer.

In this paper some of the JET diagnostics will be described. No attempt will be made to describe all the systems listed in table 1 but a few typical systems will be selected to illustrate the range of measurements and the different techniques that are used.

MAGNETIC MEASUREMENTS

Measurements of the poloidal magnetic field outside the plasma are used to determine the discharge current, loop volts, ohmic power input, position and shape of the plasma boundary (Stott 1982). More detailed analysis of the data yields information on the total plasma energy and pressure, plasma inductance and the shape of the magnetic surfaces inside the plasma. The magnetic measurement coils are shown in figure 3. The component of the poloidal magnetic field perpendicular to the surface of the vacuum vessel is measured with a set of flux loops. There are two types of loops on the outer surface of the vacuum vessel: full flux loops that make a single turn in the toroidal direction are used in locations where there are no obstructions from ports, etc.; saddle loops are used in places where there are obstructions. The component of the poloidal field parallel to the vacuum-vessel surface is measured with small pickup coils that are located inside inconel protection tubes on the inside of the vacuum vessel. There are 18 of these coils distributed around the poloidal circumference and there is an identical set of coils on each of the octants. The signals from these coils are processed electronically and combined in various ways by using both analogue and digital techniques to yield the various plasma quantities. For example, the plasma current is obtained by adding the signals from all the internal pickup coils to simulate a continuous Rogowski coil. The plasma position and the shape of the outermost magnetic flux surface are determined to a typical accuracy of ± 10 mm by a numerical solution of the Laplace equation for the poloidal field outside the plasma with the boundary conditions fitted to the field components measured by the magnetic diagnostics. The

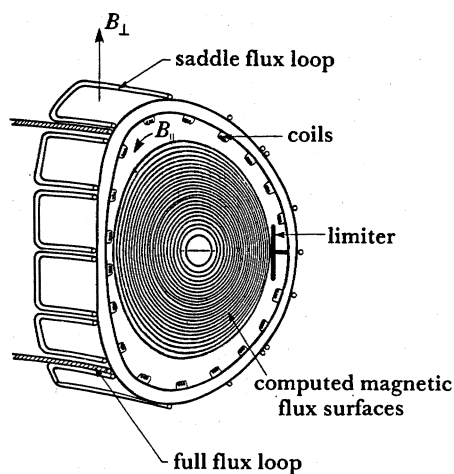


FIGURE 3. Magnetic diagnostics.

flux surfaces inside the plasma can be estimated by solving the Grad–Shafranov equation, and the integral plasma quantities such as total kinetic energy, pressure and inductance are obtained from the Shafranov integrals (Mukhovatov & Shafranov 1971).

The plasma pressure is also determined by the diamagnetic effect on the toroidal magnetic field, which is measured by coils mounted on one of the toroidal-field coils.

ELECTRON DENSITY

As in most other tokamaks the electron density n_e is measured by interferometry with microwave and far-infrared radiation. The refractive index η of an ordinarily polarized electromagnetic wave (i.e. with the \mathbf{E} vector of the wave parallel to the tokamak's \mathbf{B} field) is a function of the local electron density. Thus $\eta = (1 - n_e/n_c)$, where $n_c = 4\pi^2 c^2 \epsilon_0 m_e / \lambda^2 e^2$ is the cut-off density for propagation of the probing beam of wavelength λ . The microwave interferometer operates at a wavelength of 2 mm along a vertical chord through the major radius $R = 3.12$ m. The phase change in the transmitted beam because of the density-dependent refractive index of the plasma is compared with the phase of a reference beam that has traversed a similar path length in air. The number of interference fringes is counted electronically and at this wavelength one fringe is equivalent to a change in plasma density integrated along the chordal line of sight of *ca.* 10^{20} m^{-2} . Thus the single channel interferometer measures the integral of density times distance along the line of sight. To determine spatial profiles of the density we need to make simultaneous measurements along a number of different chords. If the poloidal cross section is circular, the density profile is then obtained from the line-integral measurements by Abel inversion. However, if the poloidal cross section is non-circular, as in JET, it is necessary either to make measurements along orthogonal chords and use tomographic methods, or to assume that the surfaces of constant density coincide with the magnetic flux surfaces measured by magnetic diagnostics. The main interferometer on JET (figure 4) has seven vertical and three lateral lines of sight (Veron 1982). The system works at a wavelength of $195 \mu\text{m}$ with a DCN laser. The shorter wavelength is not refracted as strongly as the microwave beam and this system can thus operate at higher densities. A problem with all interferometers, particularly those operating at short wavelengths, is that any mechanical vibrations of the optical components also produce changes in the optical path length that are indistinguishable from plasma-density changes. The optical components of the vertical channels are mounted on a

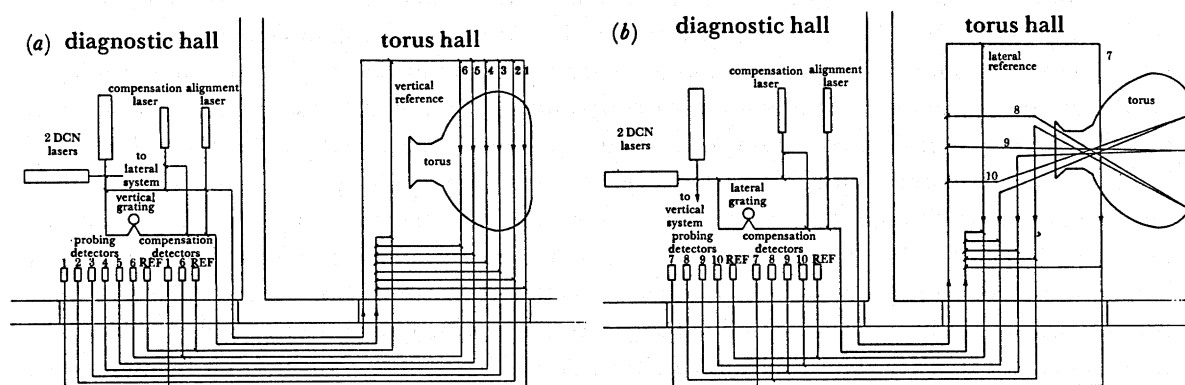


FIGURE 4. Schematic of the multichannel interferometer. (a) vertical channels, (b) lateral channels. (Compensation is only required for lateral system.)

massive support frame that is mechanically independent of the rest of the JET machine but some of the components on the lateral channels cannot be so isolated and are thus sensitive to vibrations. The horizontal channels have been designed to operate simultaneously with a second wavelength ($\lambda = 3.39 \mu\text{m}$) that is affected more strongly by the mechanical vibrations than the main wavelength ($\lambda = 195 \mu\text{m}$). However, this system has not proved satisfactory because of technical difficulties with the internal mirrors at the shorter wavelength and the second wavelength is being changed to $119 \mu\text{m}$.

An alternative method of density measurement that is being developed on JET is reflectometry, where a microwave beam directed into the plasma is reflected at the cut-off density (Hubbard *et al.* 1987; Simonet 1985). This technique is particularly suitable for measurements near to the edge of the discharge and for studying temporal fluctuations in the density.

ELECTRON TEMPERATURE

The traditional method of measuring electron temperature in tokamaks is Thomson scattering. An incident beam of laser light is scattered and Doppler-shifted by the electrons in the plasma. The scattered light is thus broadened in wavelength by an amount that corresponds to the velocity distribution of the electrons, and the temperature can be determined directly. This technique has a special place in the history of tokamak research, because its successful use by a joint British and Russian team on the T3 tokamak in Moscow in 1969 confirmed that tokamaks had high electron temperatures (Peacock *et al.* 1968), and this stimulated a rapid development of tokamak research outside the U.S.S.R.

JET will have two Thomson-scattering systems, one is already operating and the second is under construction. The first system (Nielson 1982), which we call the 'single-point Thomson-scattering system' is of conventional geometry i.e. the scattered light is collected in a cone at 90° to the incident light. A schematic is shown in figure 5. A ruby laser is used as the source and can be operated in a variety of combinations of energy per pulse and repetition rate ranging from a single pulse of 25 J to a series of pulses of 2.5 J at 1 Hz. The laser is located on the roof of the JET torus hall as shown in the schematic. The beam passes into the torus hall through a labyrinth to shield against neutrons, and into the torus through a quartz vacuum window. The scattered light leaves the torus through a cluster of seven windows each *ca.* 200 mm diameter that are arranged to have an effective aperture equivalent to that of a single window *ca.* 500 mm diameter. The light is collected by a large reflecting telescope and directed into the roof laboratory where the scattered spectrum is dispersed by a large prism spectrometer onto an array of photomultipliers. The Thomson-scattering diagnostic has the advantage that the local electron temperature is measured directly and unambiguously for the electron velocity distribution in a well-defined volume of plasma (typically $5 \text{ m} \times 1 \text{ m} \times 1 \text{ m}$) at the well-defined instant when the laser is fired. It is, however, limited to a single spatial point measurement per discharge, (although the system can be moved to different major radii in between discharges) and to a maximum repetition rate of one measurement per second. The accuracy is determined principally by the number of scattered photons. For typical JET discharge conditions, an absolute accuracy of $\pm 10\%$ can be obtained with a laser pulse *ca.* 5 J at a repetition rate of 0.5 Hz. The accuracy can be improved if necessary (for example in low-density plasmas) by increasing the laser energy (ultimately to a single pulse of 20 J) at the expense of repetition rate, or if required the repetition rate can be increased to 1 Hz with a laser energy of 2.5 J per pulse at the expense of slightly reduced accuracy.

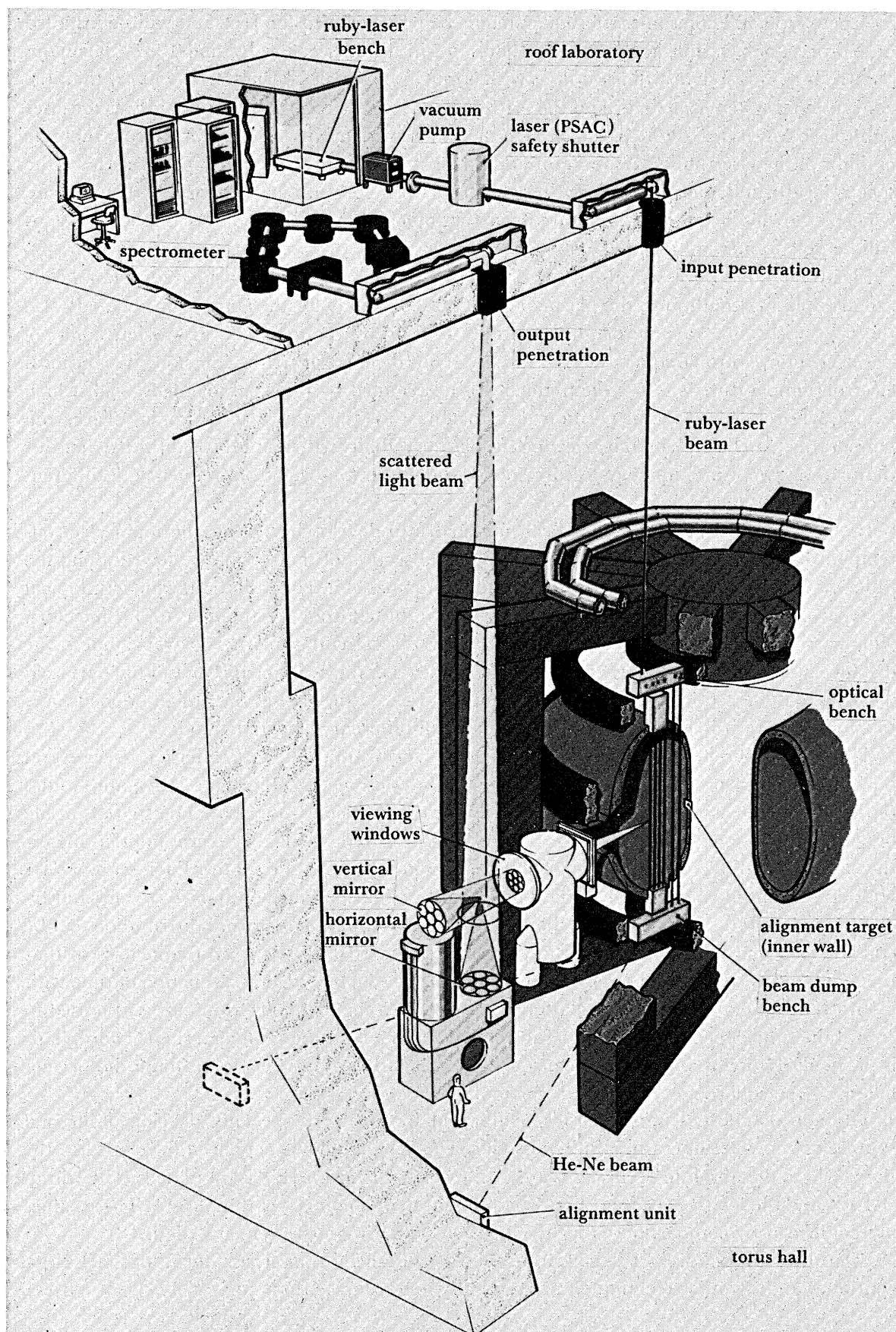


FIGURE 5. Schematic of the single-point Thomson-scattering diagnostic.

A new type of Thomson-scattering system is being developed for JET and will be installed in a provisional version at the end of 1986, and in a final version by mid-1987 (Salzmann *et al.* 1985). This system will use a laser with a much shorter pulse length (*ca.* 250 ps) than the conventional system (*ca.* 20 ns) and the scattered light will be recorded continuously as the laser light pulse travels across the plasma. Then the spatial profile will be determined from the time of flight of the laser pulse. Temperature and density will be determined respectively from the spectral width and intensity of the scattered light as in the conventional system. This new system, which is shown schematically in figure 6, will use much of the existing optics and both systems will be able to operate together.

Electron temperatures can also be measured by electron-cyclotron emission (ECE). For a wide range of plasma conditions, the plasma emits as a black body for the extraordinary mode (i.e. the \mathbf{E} vector of the wave perpendicular to the \mathbf{B} vector of the tokamak) at low harmonics of the electron-cyclotron frequency $\omega_{ce} = eB/m_e c$. Thus the intensity of the emission gives the local electron temperature whereas the frequency is determined by the local magnetic field, which is uniquely related to radial position in a tokamak. In this way spatial profiles of electron temperature can be measured by viewing the plasma radially with a suitably calibrated detector that can be swept in frequency to correspond to the electron-cyclotron frequency at different radii along the line of sight.

In JET, considerable effort has been invested into developing ECE as the main electron-temperature diagnostic (Costley 1982). A poloidal section of the plasma is viewed along ten different chords by an array of rectangular horn antennas. The ECE radiation, which for typical JET parameters is in the range 70–350 GHz is transmitted from the antennas to the detectors, which are located outside the torus hall, by oversized rectangular microwave waveguides. The distance along the route followed by the waveguides is of the order of 100 m and the oversized waveguide is needed for low attenuation, but great care is needed in the design of bends, etc. to avoid serious problems with conversion between different waveguide modes.

Three types of detector are used. The complete spectrum of the ECE radiation over several harmonics is measured with scanning Michelson interferometers, and the relative amplitudes of the different harmonics are used to check that the emission is thermal. The spatial profile of temperature along different chords (figure 7) is measured with Fabry–Perot interferometers that are scanned over the second-harmonic emission in a time of *ca.* 3 ms. Each scan gives a temperature profile along the chordal line of sight with a spatial resolution *ca.* 10 cm, and by combining the data from different chords a two dimensional temperature distribution can be constructed. The Fabry–Perot instruments can be operated also at fixed frequencies so that the temperature at a selected position in the plasma can be recorded as a function of time with a sensitivity *ca.* 5 eV and time resolution *ca.* 10 μ s. A 12-channel polychromator is also used to record the time dependence of temperatures at 12 selected positions along a single chord. This is particularly useful for measurements of the propagation of heat waves through the plasma following the collapse of an internal ‘sawtooth’ instability.

The ECE diagnostics are absolutely calibrated by means of specially developed thermal sources of known temperature and emissivity. This technique has now been developed to the point where the absolute accuracy of the ECE measurements on JET is estimated to be within $\pm 10\%$ and the relative accuracy between different spatial points is within $\pm 5\%$. These values are confirmed by comparison with the Thomson-scattering measurements (figure 8).

Electron temperatures deduced from Si–Li pulse-height analysis (PHA) of soft-X-ray continua, and by other techniques, are generally less accurate than ECE.

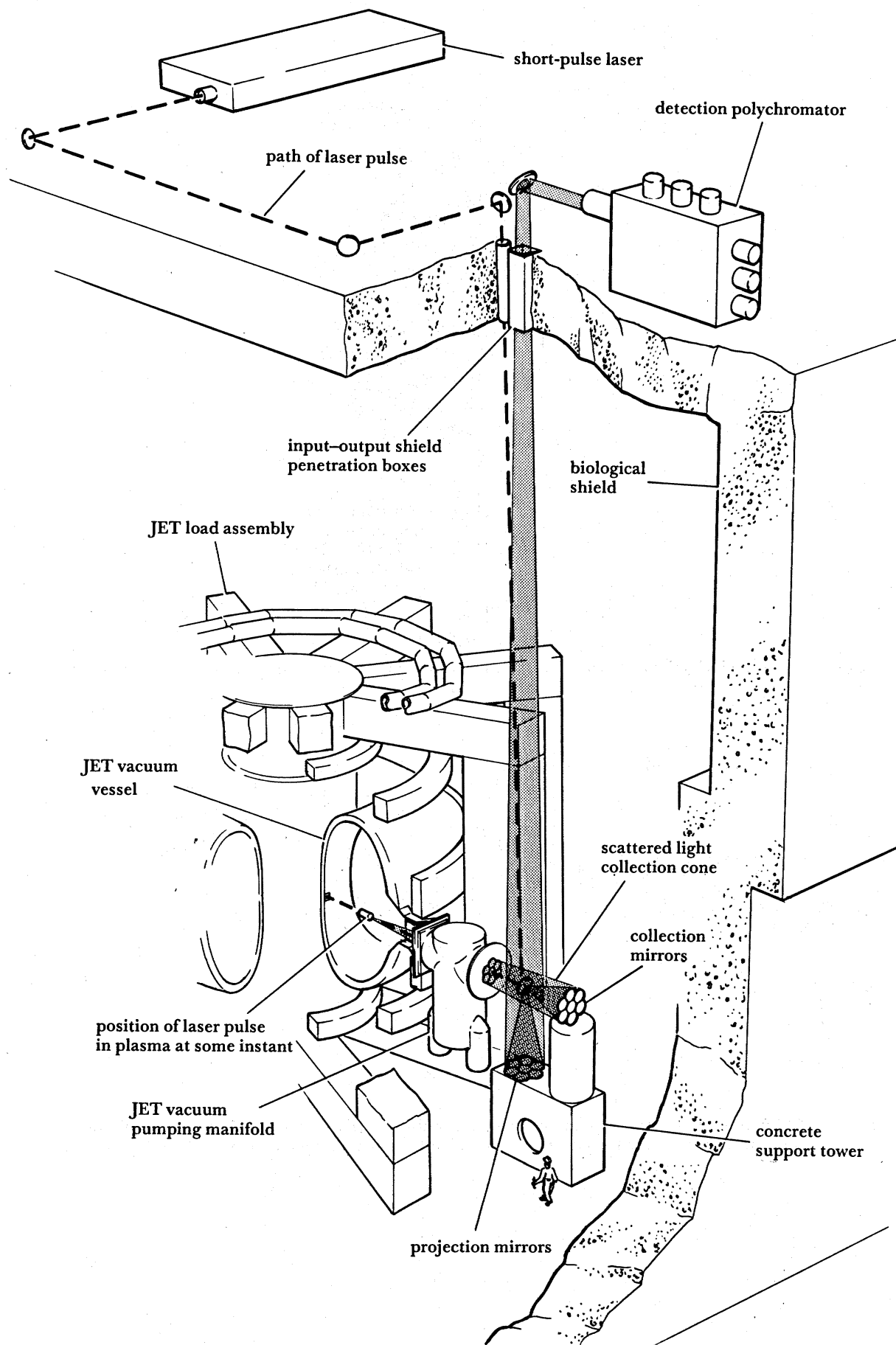


FIGURE 6. Schematic of the LIDAR Thomson-scattering system.

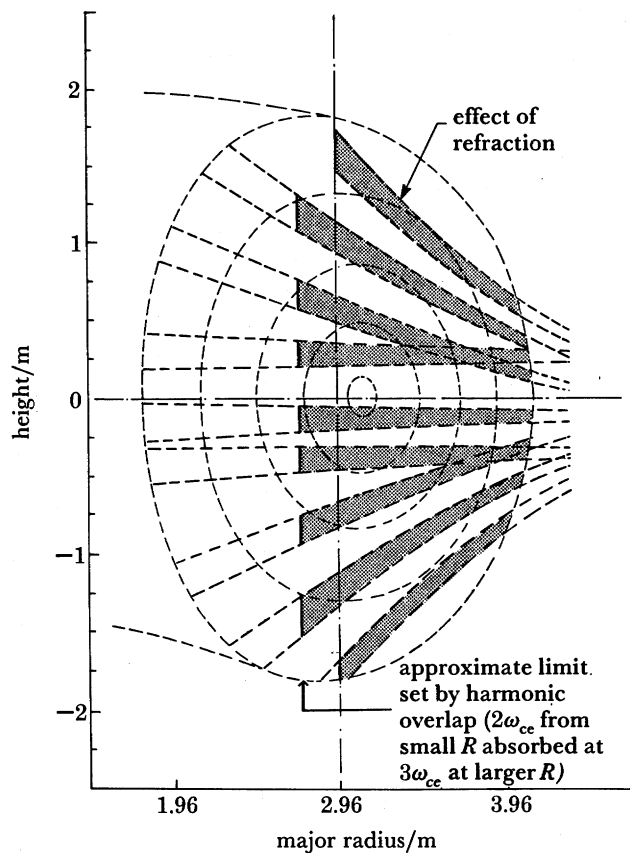


FIGURE 7. The multichord ECE system. The shaded areas show the regions of the plasma covered by the ECE measurements.

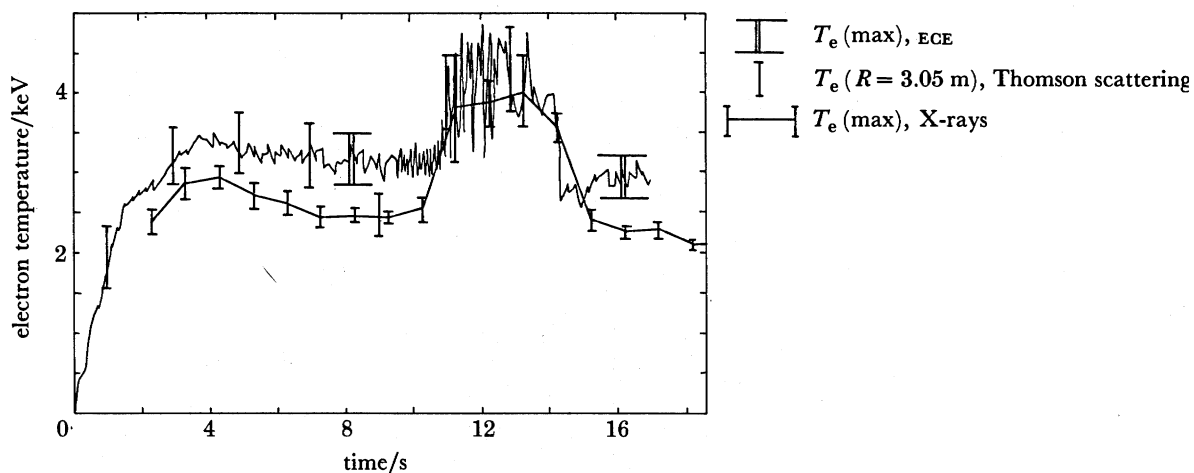


FIGURE 8. Comparison of electron temperatures measured by different JET diagnostics. The data from the different diagnostics are all based on independent absolute calibrations and have not been normalized in any way.

ION TEMPERATURE

In general the temperatures of the ions in a tokamak are different from that of the electrons. In ohmically heated discharges the primary power input is via the electrons, and thus they are hotter than the ions, whereas in discharges with powerful additional heating of the ions the ion temperatures may be higher than that of the electrons. Generally the methods for measuring the ion temperatures have more difficulties and more limited ranges of application than the methods described above for the electrons and so this is an area where the overlap of several different diagnostics is particularly necessary.

The classic method is based on charge-exchange neutrals (Afrosimov & Kislyakov 1982). Even in these highly ionized tokamak plasmas there is a finite but small density of non-ionized neutral atoms (typically *ca.* 10^{12} – 10^{13} atoms m^{-3} in the centre of the discharge compared with ion densities in the range 10^{19} – 10^{20} ions m^{-3}). Charge-exchange collisions between these neutrals and plasma ions produce neutrals with energies equal to those of the plasma ions but able to escape from the confining magnetic fields. The flux of these neutrals is small (typically 10^{14} atoms m^{-2} Sr^{-1} keV^{-1}) and to detect them they are first reionized by a hydrogen gas-stripping cell, and then passed through magnetic and electrostatic analysers to disperse them in momentum and energy onto an array of channel-multiplier detectors. In this way the energy spectra of hydrogen and deuterium neutrals can be measured simultaneously. In small low-density plasmas the neutral energy spectrum has a characteristic shape that gives directly the ion temperature in the core of the discharge but in larger devices like JET the low neutral-atom density in the core and the strong attenuation of neutrals escaping from the large-diameter plasma introduces a severe distortion of the charge-exchange spectrum so that a simple fit to the measured spectrum underestimates the central temperature. Transport code calculations are used to extrapolate to the central temperature. The neutral-particle diagnostic system on JET has an array of five analysers viewing along different chords in the poloidal section, and the whole array can be scanned to view in different toroidal directions.

Neutron diagnostics are also used to measure ion temperatures in deuterium plasmas (Jarvis *et al.* 1987). The neutron yield from a deuterium plasma with a Maxwellian-ion distribution is proportional to the square of the deuteron density and to a high power of the ion temperature. Thus the neutron yield is *ca.* $n_d^2 T_i^\gamma$, where $4 < \gamma < 5$ for $T_i < 10$ keV. The neutron yield is dominated by the hot central core of the plasma and is relatively insensitive to the precise shape of the density and temperature profiles provided that they are not too extreme. The ion temperature in the core of the discharge can therefore be deduced from the total neutron yield provided the deuteron density is known and the ions are Maxwellian. The latter requirement is usually met in ohmically heated plasmas but is usually violated with powerful additional heating of the ions that results in a non-Maxwellian velocity distribution.

However, a more direct measurement of the ion temperature can be obtained by neutron spectrometry. The energy distribution of the neutrons is broadened about the fusion energy (2.4 MeV for D–D and 14.1 MeV for D–T) by the energy of the interacting ions. The broadening is relatively small ($\Delta E/E \lesssim 5\%$) and therefore very good energy resolution is needed for a neutron spectrometer. Good shielding and collimators are needed to reduce the background of lower energy neutrons which have been scattered from the material structures surrounding the plasma. The spectrometers also need to cover a very wide dynamic range of neutrons yields from typically 10^{12} neutrons s^{-1} in low-temperature deuterium plasmas to

typically 10^{19} neutrons s^{-1} in high-temperature deuterium–tritium mixtures. There is no single-detector technique that will cover this wide range of fluxes with adequate energy resolution and thus JET has built several different instruments to cover the expected range. At low yields in deuterium plasmas we have used ^3He ionization chambers located on the roof of the torus hall with the penetration hole through the roof as a collimator. A typical spectrum is shown in figure 9. At higher fluxes in deuterium plasmas we will use a variety of other methods including a novel time-of-flight technique that uses a pair of scintillators. Simultaneous measurement of the total neutron yield and of the ion temperature by a neutron spectrometer allows the determination of the deuteron density, which is generally significantly less than the electron density (typically $n_d/n_e \sim 0.5$) because of the dilution by impurities.

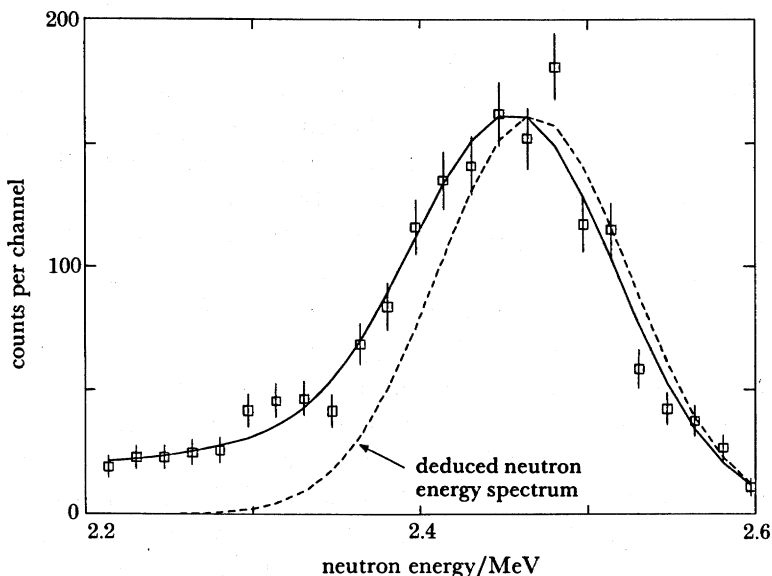


FIGURE 9. Typical spectrum of neutrons emitted from a deuterium plasma. $T_i = 2.68 \pm 0.17$ keV.

A typical comparison between the temperatures measured by the charge exchange and neutron diagnostics is shown in figure 10. In this case the ion temperature was relatively low and the neutron spectrum had to be integrated for 6 s during the flat-top phase of the discharge for good statistics, but more recent experiments with higher temperatures have allowed the time resolution to be reduced to about 1 s. In the example shown there is good agreement between the different measurements, but this is not always so, and in some discharge conditions there may be significant differences between the different measurements. The main source of difficulty is that all these methods are very sensitive to distortions of the high-energy tail of the ion-energy distribution, and in many cases the ions are no longer Maxwellian and therefore the simple concept of a plasma temperature is no longer valid. A particularly important quantity is the difference between the ion and electron temperatures that determines the coupling between the two species and is required for a detailed analysis of the energy balance. However, in high-density plasmas when the coupling is strong the difference in temperatures may be comparable to the accuracy (typically $\pm 10\%$ for T_e and $\pm 20\%$ for T_i) of the measurements, and thus the relative accuracy of the temperature difference (and hence the coupling) is poor.

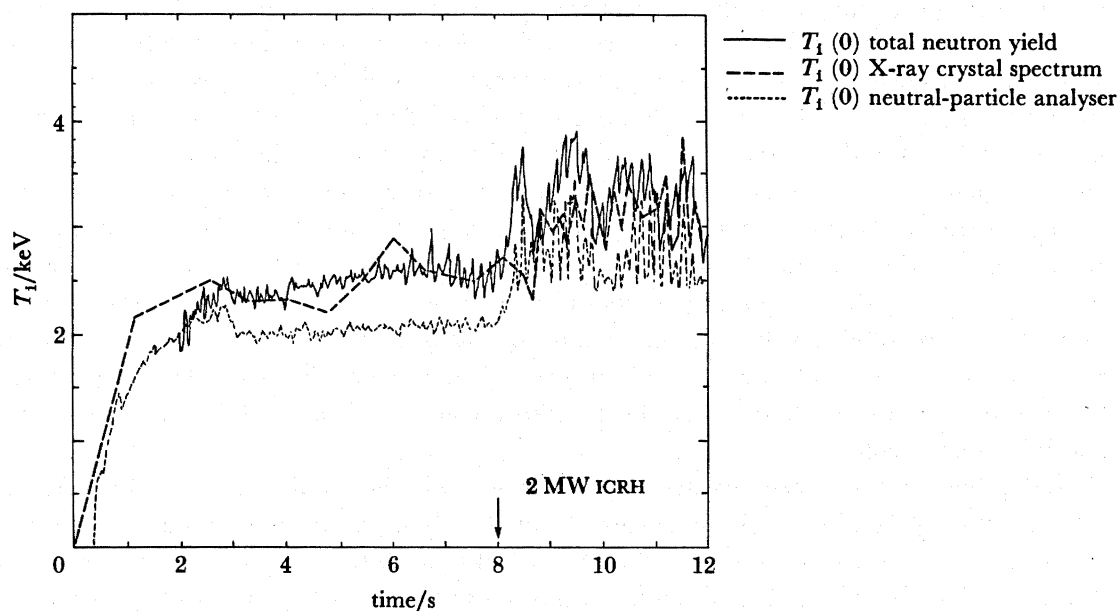


FIGURE 10. Comparison of ion temperatures measured with different methods. The data from the different diagnostics are all based on independent absolute calibrations and have not been normalized in any way.

Ion temperatures are also measured from the line widths of impurity emission lines. The impurity ions are of course in good thermal equilibrium with the hydrogenic ions and thus the measured impurity ion temperatures can be related to the hydrogenic ion temperatures. These measurements can be made in different parts of the spectrum. In the X-ray region we use a high-resolution crystal spectrometer to observe highly ionized stores of nickel from the centre of the plasma. The crystal and detector (a multiwire proportional counter) are located outside the torus hall behind the main radiation shield wall so that this system is hardened against neutrons and γ -rays. The first results are now being obtained with this system, which can be used to measure bulk rotation of the plasma as well as temperatures.

IMPURITY DIAGNOSTICS

As discussed in the accompanying paper by Engelhardt (this symposium) tokamaks are contaminated by impurities as a result of the interaction between the plasma and the surrounding material surfaces. Various diagnostic methods including spectroscopy are used to determine the processes that lead to this contamination and to study the effects of impurities in the plasma.

Spectroscopic diagnostics are the main methods for identifying the impurities in the plasma and for measuring their concentrations. The impurities are characterized by spectral line emissions over a very wide range from the visible (*ca.* 6000 Å†) through the ultraviolet to the soft X-ray region (*ca.* 1 Å). Different instruments are needed to cover this very wide range. The resonance lines of the important low- Z impurities (oxygen and carbon) and the lower ionization stages of the high Z impurities (nickel) are in the ultraviolet region and it is this region of the spectrum which has traditionally been used for quantitative measurements in smaller tokamaks.

† Å = 10^{-10} m.

Unfortunately spectrometers in this part of the spectrum need to be placed in direct line of sight of the plasma as the reflectivity of mirror surfaces is very low and, as there are no suitable window materials below *ca.* 1400 Å, these instruments must be directly coupled to the tokamak vacuum system. The main system that has been built for JET will cover the wavelength range from 2000 to 100 Å and is based on three identical duochromators. The plasma is viewed via grazing-incidence mirrors that can be rotated to give a spatial scan of the plasma cross section. Two instruments are mounted horizontally, each viewing one half of the plasma, whereas the third instrument views vertically. In this way it is intended to be able to unfold poloidally asymmetric impurity distributions by tomographic inversion. These instruments gave the first data at the end of 1985, but because of vacuum problems in the rotary mechanisms the full implementation is likely to be delayed. There are subsidiary vacuum ultraviolet spectrometers at longer (i.e. greater than 2000 Å) and shorter (20–100 Å) wavelengths which view the plasma along fixed lines of sight.

Considerable effort has been invested into spectroscopy in the visible (i.e. 6000–3000 Å) and soft X-ray (20–1 Å) regions of the spectrum because for both, light relay systems can be used to place the spectrometers outside the radiation-shielding wall. In the visible region this is done with fibre optics whereas in the soft X-ray region a crystal spectrometer with two crystals in a periscope type arrangement is being built. Quantitative interpretation of the emission lines in the visible is more difficult, but in JET considerable use has been made of these techniques to view the limiter and walls and thus determine the fluxes of hydrogen and impurities which enter the plasma.

More direct measurements of the plasma interaction with material surfaces has been made by surface analysis of samples removed from the limiter and walls whenever the JET vacuum vessel has been opened for maintenance. These measurements necessarily give only an integrated picture over many months of operation, but probe drive systems are now being installed that will allow sample surfaces to be exposed near to the walls and limiters, and then transferred promptly under vacuum to an analysis system where a variety of surface analytical methods can be used. The same probe drive systems are also used to introduce electrical probes into the boundary regions of the discharge to measure the local plasma density and temperatures. These plasma data are required to interpret the spectroscopic measurements of impurity influxes at the plasma edge.

The degree of impurity contamination in tokamak plasmas is usually expressed by the average ionic charge $Z_{\text{eff}} = \sum_i n_i Z_i^2 / n_e$, where n_i is the density of impurity ions with charge Z_i and the summation is taken over all impurity charge states. In JET we measure Z_{eff} by several methods including the enhancement of the continuum radiation from bremsstrahlung in a region of the visible spectrum where there are no strong emission lines, and from the enhancement of the continuum in the soft-X-ray region. Generally there is agreement to within an accuracy of about 20% between these spectroscopic measurements of Z_{eff} , with values of Z_{eff} derived from the plasma-resistance enhancement.

The power radiated by impurities is measured by arrays of bolometers that view the plasma in orthogonal directions through small apertures. The horizontal camera has 20 channels and the vertical camera has 14 channels. Each detector consists of a pair of thin-film gold resistors evaporated onto a mylar foil. One resistor receives plasma radiation and the other is shielded. The pair are connected in a bridge arrangement to cancel drifts in the substrate temperatures.

The temperatures of the surfaces of the limiters, RF antennas and vulnerable areas of the vacuum-vessel wall are monitored with infrared television cameras. One system is based on

charge-coupled device (CCD) cameras and has good spatial resolution. It is sensitive to radiation *ca.* $1\ \mu\text{m}$ wavelength and has a minimum temperature threshold *ca.* $700\ ^\circ\text{C}$. It is used primarily to monitor these surfaces for localized heating due to plasma interaction, although some information about limiter power fluxes can also be determined. The second system has low spatial resolution but operates at longer wavelengths (*ca.* $3\text{--}5\ \mu\text{m}$) and thus is sensitive to lower surface temperatures and can be used for more accurate power-flux measurements.

FLUCTUATIONS

The discussion of JET diagnostics so far has concentrated on the measurement of quasi-stationary plasma parameters, but most of these systems also have the capability to follow non-stationary plasma phenomena. Of particular interest at the moment in JET are the periodic density and temperature oscillations in the core of the discharge, usually called 'sawteeth', and the complex chain of internal magnetohydrodynamic oscillations that precede the catastrophic termination of the discharge known as a 'disruption'. Among the most useful of the systems described already are the ECE and magnetic diagnostics which have very good time resolution and sensitivity to record these events.

A diagnostic which has been installed on JET specifically to record these internal transitory phenomena is the X-ray diode-array system (Edwards *et al.* 1987). Small semiconductor diode detectors are sensitive to soft X-rays emitted from the plasma and can therefore detect small localized temperature fluctuations. They are mounted inside the JET vacuum vessel in two arrays viewing the plasma cross section in orthogonal directions as shown in figure 11. The wavelength range of the system can be changed by filters that can be introduced in front of

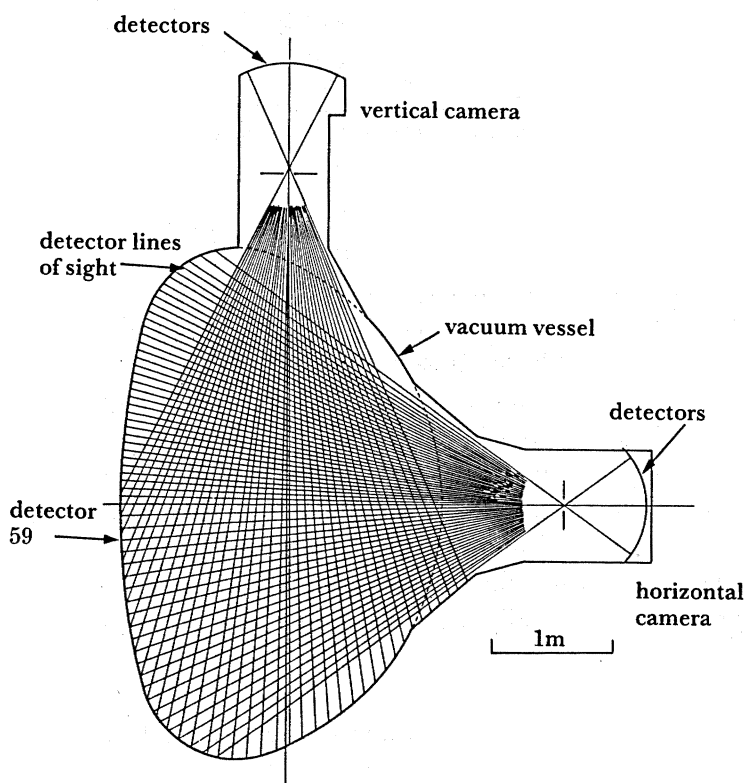


FIGURE 11. Soft-X-ray diode arrays.

the detectors and this has the effect of changing the sensitivity of the system to correspond to changes in plasma temperature. Each detector of course integrates the emission along its line of sight but with such a large number of sight lines (62 horizontal and 38 vertical) it is possible to unfold the integral signals numerically using tomographic methods to produce contour maps of the local emission density. This diagnostic has proved particularly powerful in observing the mechanism of the sawtooth oscillation. An example is shown in figure 12; it shows how the sawtooth collapse takes place on a very short time scale (less than $100 \mu\text{s}$) and appears to involve a rapid outward convection of the hot core of the discharge often without any prior MHD activity. These measurements have substantially changed the understanding of the sawtooth that had been widely accepted and provide a clear example of the need for fusion experiments like JET to be well diagnosed.

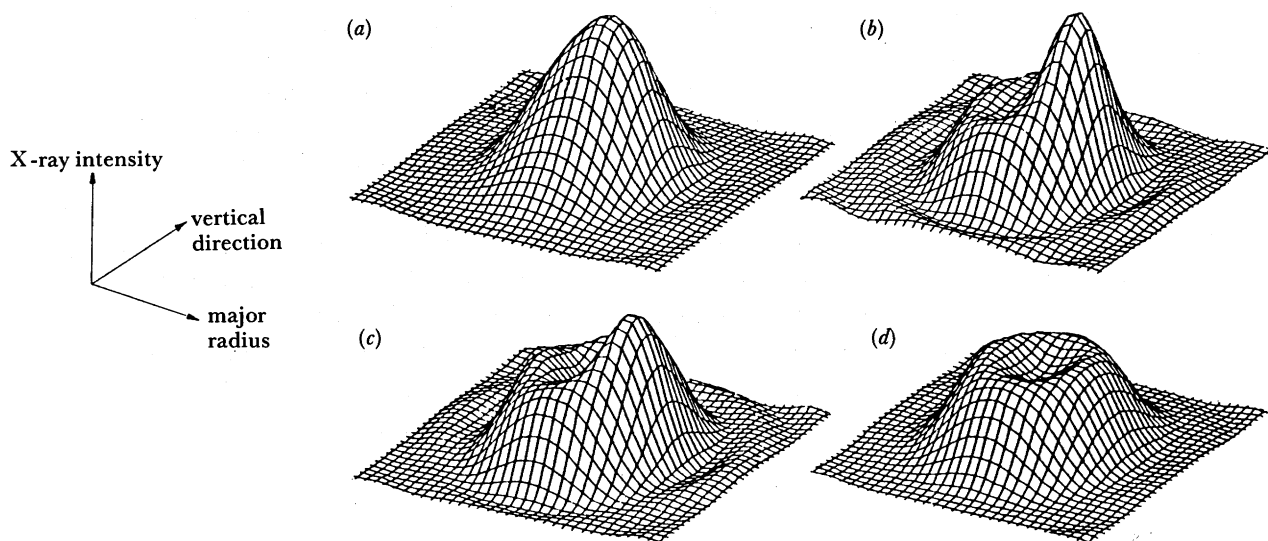


FIGURE 12. X-ray emission during a sawtooth crash. (a) initial state $t = 0$; (b) hot spot moves rapidly $t = 126 \mu\text{s}$; (c) hot spot collapses $t = 200 \mu\text{s}$; (d) stable final state $t = 1930 \mu\text{s}$.

CONCLUSIONS

A considerable effort has been invested into providing the JET experiment with a comprehensive set of diagnostics. Particular emphasis has been placed on making measurements of the different plasma parameters simultaneously within a single discharge, to avoid problems of irreproducibility. Considerable care has been taken during the design and construction of these diagnostic systems to ensure that they are consistent with the high standards of engineering of the other systems of the JET machine. Many of the systems described in this paper were operated in a preliminary version for the first operation of JET in 1983, and since then they have been refined and brought into full operation. Most of these systems are now capable of reliable and automatic operation, allowing the scientific personnel to concentrate on interpretation of data. A few systems (including the neutron systems specifically intended for the later phases of JET's programme) are still in construction and will be installed within the next few years.

I acknowledge the many contributions by my colleagues in JET and the Associations to this work.

REFERENCES

- Afrosimov, V. V. & Kislyakov, A. I. 1982 *Diagnostics for fusion reactor conditions*, pp. 289–310. Brussels: Commission of the European Communities, EUR 8351–1.
- Costley, A. 1982 *Diagnostics for fusion reactor conditions*, pp. 129–166. Brussels: Commission of the European Communities, EUR 8351–1 EN.
- Edwards, A., Fahrbach, H-U., Gill, R. D., Granetz, R., Oord, E., Schramm, G., Tsuji, S., Weller, A. & Zasche, D. 1987 The JET soft X-ray diode array diagnostic. In *6th Conf. on High Temperature Plasma Diagnostics, Hilton Head Island, South Carolina, March 1986*. (*Rev. Scient. Instrum.* (In the press).)
- Hubbard, A. E., Costley, A. E. & Gowers, C. W. 1987 A simple fixed frequency reflectometer for plasma density profile measurements on JET. *J. Phys. E.* (Submitted).
- Jarvis, O. N., Gorini, G., Hone, M., Källne, J., Sadler, G., Merlo, V. & van Belle, P. 1987 Neutron Spectrometry at JET. In *Proc. 6th Conf. on High Temperature Plasma Diagnostics, Hilton Head Island, South Carolina, March 1986*. (*Rev. Scient. Instrum.* (In the press).)
- Mukhovatov, V. S. & Shafranov, V. D. 1971 *Nucl. Fusion* **2**, 605–633.
- Nielsen, P. 1982 *Diagnostics for fusion reactor conditions*, pp. 225–259. Brussels: Commission of the European Communities, EUR 8351–1 EN.
- Peacock, N. J., Robinson, D. C., Forrest, M. J., Wilcock, P. D. & Sannikov, V. V. 1968 *Nature, Lond.* **224**, 448.
- Salzmann, H., Hirsch, K., Gruber, J., Röhr, H., Bredelow, G. & Witte, K. 1985 *Rev. Scient. Instrum.* **56**, 1030.
- Simonet, F. 1985 Measurement of electron density profile by microwave reflectometry on tokamaks. *Rev. Scient. Instrum.* **56** (5), 664.
- Stott, P. E. 1982 *Diagnostics for fusion reactor conditions*, pp. 403–418. Brussels: Commission of the European Communities, EUR 8351–1 EN.
- Veron, D. 1982 *Diagnostics for fusion reactor conditions*, pp. 199–224. Brussels: Commission of the European Communities, EUR 8351–1 EN.

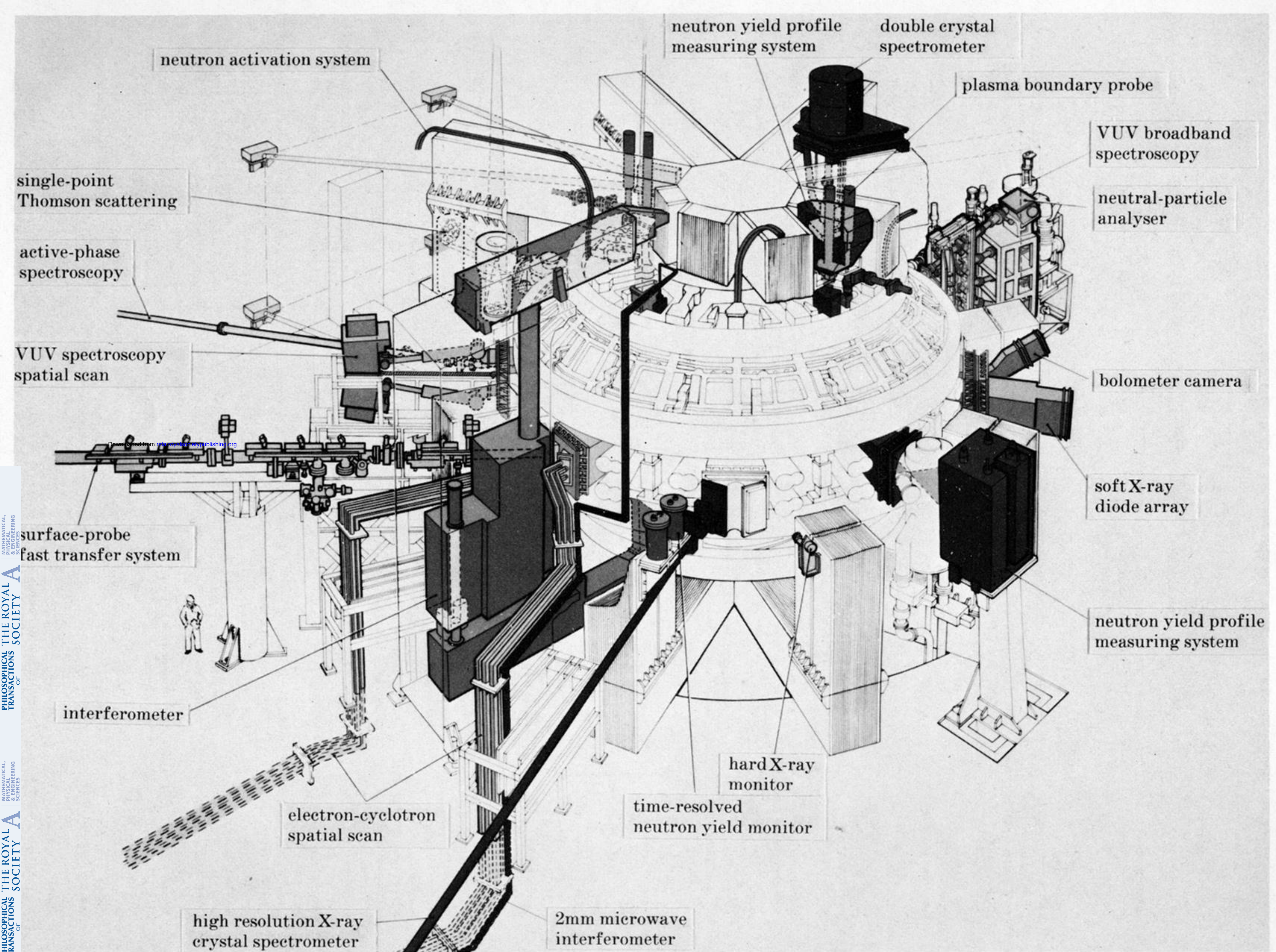


FIGURE 2. Schematic showing the location of JET diagnostic systems.

Downloaded from rsta.royalsocietypublishing.org

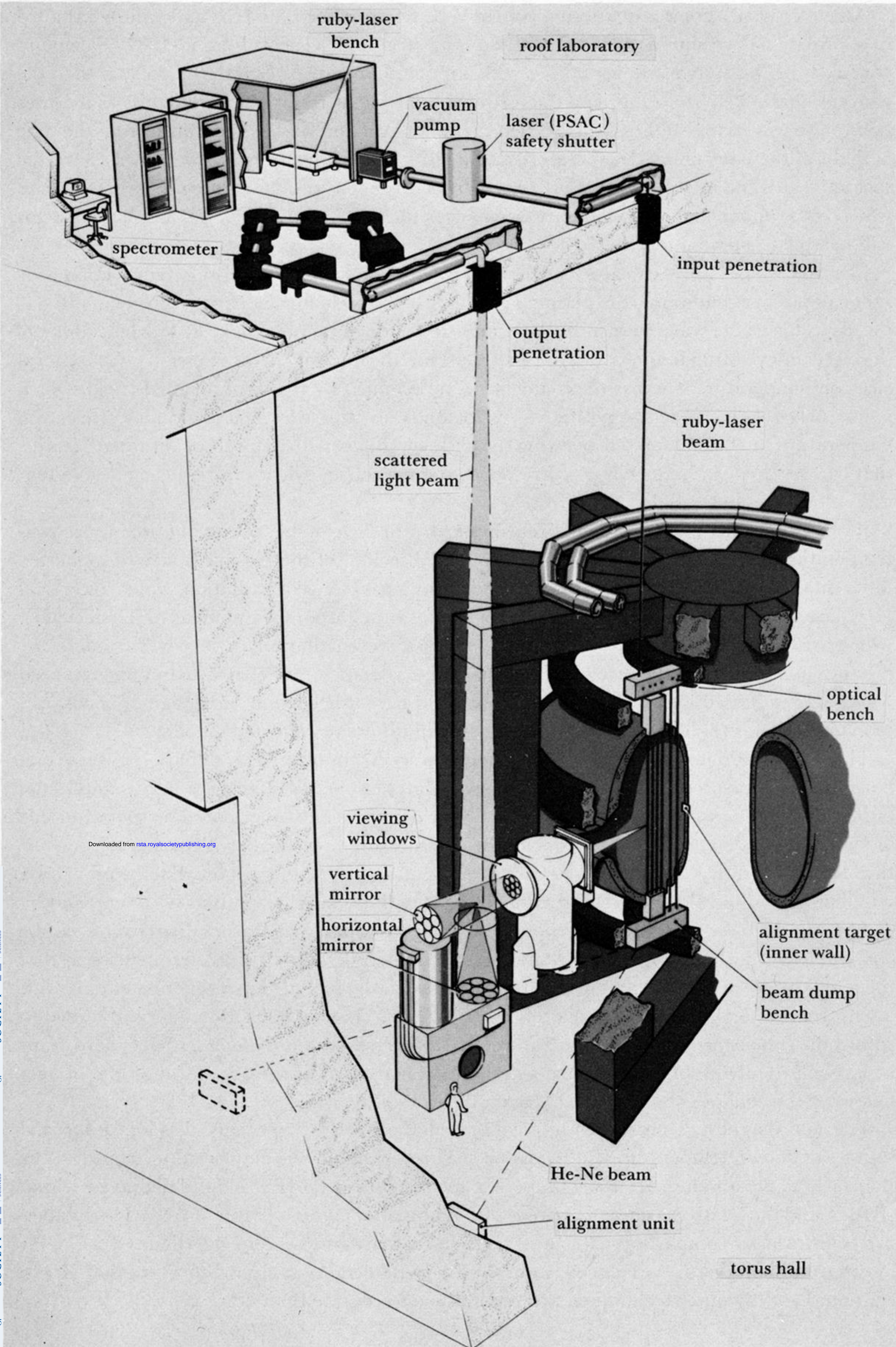


FIGURE 5. Schematic of the single-point Thomson-scattering diagnostic.